Journal of Asian Earth Sciences 85 (2014) 140–153

Contents lists available at ScienceDirect

Journal of Asian Earth Sciences

journal homepage: www.elsevier.com/locate/jseaes

Fluid inclusion, rare earth element geochemistry, and isotopic characteristics of the eastern ore zone of the Baiyangping polymetallic Ore district, northwestern Yunnan Province, China

Caixia Feng [a,*], Xianwu Bi [b], Shen Liu [a], Ruizhong Hu [b]

[a] State Key Laboratory of Continental Dynamics and Department of Geology, Northwest University, Xi'an 710069, China
[b] State Key Laboratory of Ore Deposit Geochemistry, Institute of Geochemistry, Chinese Academy of Science, Guiyang 550002, China

ARTICLE INFO

Article history:
Received 6 July 2013
Received in revised form 15 January 2014
Accepted 20 January 2014
Available online 31 January 2014

Keywords:
Fluid inclusions
Rare earth elements
Stable isotopes
Eastern ore zone
Baiyangping polymetallic ore district
Yunnan Province

ABSTRACT

The Baiyangping Cu–Ag polymetallic ore district is located in the northern part of the Lanping–Simao foreland fold belt, which lies between the Jinshajiang–Ailaoshan and Lancangjiang faults in western Yunnan Province, China. The source of ore-forming fluids and materials within the eastern ore zone were investigated using fluid inclusion, rare earth element (REE), and isotopic (C, O, and S) analyses undertaken on sulfides, gangue minerals, wall rocks, and ores formed during the hydrothermal stage of mineralization. These analyses indicate: (1) The presence of five types of fluid inclusion, which contain various combinations of liquid (l) and vapor (v) phases at room temperature: (a) H_2O (l), (b) H_2O (l) + H_2O (v), (c) H_2O (v), (d) C_mH_n (v), and (e) H_2O (l) + CO_2 (l), sometimes with CO_2 (v). These inclusions have salinities of 1.4–19.9 wt.% NaCl equivalents, with two modes at approximately 5–10 and 16–21 wt.% NaCl equivalent, and homogenization temperatures between 101 °C and 295 °C. Five components were identified in fluid inclusions using Raman microspectrometry: H_2O, dolomite, calcite, CH_4, and N_2. (2) Calcite, dolomitized limestone, and dolomite contain total REE concentrations of 3.10–38.93 ppm, whereas wall rocks and ores contain REE concentrations of 1.21–196 ppm. Dolomitized limestone, dolomite, wall rock, and ore samples have similar chondrite-normalized REE patterns, with ores in the Huachangshan, Xiaquwu, and Dongzhiyan ore blocks having large negative δCe and δEu anomalies, which may be indicative of a change in redox conditions during fluid ascent, migration, and/or cooling. (3) $\delta^{34}S$ values for sphalerite, galena, pyrite, and tetrahedrite sulfide samples range from −7.3‰ to 2.1‰, a wide range that indicates multiple sulfur sources. The basin contains numerous sources of S, and deriving S from a mixture of these sources could have yielded these near-zero values, either by mixing of S from different sources, or by changes in the geological conditions of seawater sulfate reduction to sulfur. (4) The C–O isotopic analyses yield $\delta^{13}C$ values from ca. zero to −10‰, and a wider range of $\delta^{18}O$ values from ca. +6 to +24‰, suggestive of mixing between mantle-derived magma and marine carbonate sources during the evolution of ore-forming fluids, although potential contributions from organic carbon and basinal brine sources should also be considered. These data indicate that ore-forming fluids were derived from a mixture of organism, basinal brine, and mantle-derived magma sources, and as such, the eastern ore zone of the Baiyangping polymetallic ore deposit should be classified as a "Lanping-type" ore deposit.

1. Introduction

The Baiyangping Cu–Ag polymetallic ore district is located in the northern segment of the Lanping–Simao Basin of southwest China, is subdivided into eastern and western ore zones, and contains estimated reserves of 32 Mt Cu, 4149 t Ag, 23 Mt Pb, 18 Mt Zn, and 1444 t Co (Third Geology and Mineral Resources Survey, 2003). The eastern (or Sanshan–Hexi) ore zone is the second largest ore district in the Lanping Basin, and has estimated reserves of ~0.3 Mt Cu, >3000 t Ag, and >0.5 Mt Pb + Zn at grades of 1.6–3.3% Zn, 0.81–3.55% Pb, and 23.3–220.1 g/t Ag (Third Geology and Mineral Resources Survey, 2003; He et al., 2009). The eastern ore zone hosts 15 economic orebodies; these orebodies host mineralization within veins and lenses, and as finely-stratified and irregular bodies, and are 200–1000 m long and 2–8 m thick (Third Geology and Mineral Resources Survey, 2003; Liu et al., 2010).

* Corresponding author. Tel.: +86 29 88302226.
E-mail address: fengcaixia@vip.gyig.ac.cn (C. Feng).

http://dx.doi.org/10.1016/j.jseaes.2014.01.019
1367-9120/

Previous studies of the eastern ore district have focused on geochemistry (Tian, 1997, 1998; He et al., 2005), structural controls on mineralization (Shao et al., 2002; Xue et al., 2002a; He et al., 2004a), isotope geochemistry (Chen et al., 2000; Li et al., 2004), fluid geochemistry (Gong et al., 2000; Xue et al., 2002b; He et al., 2004b; He et al., 2005, 2009), and Ag, Co, Ni, and Bi occurrences within orebodies in the district (Liu et al., 2010). However, the source of ore-forming fluids and metals in the study area is still controversial, with a number of previously proposed hypotheses for sources of ore-forming fluids, including deep, hot brines (Chen et al., 2000), meteoric and formation water (Yang et al., 2003), early- and late-stage ore-forming fluids originating from a deep CO_2-bearing basin containing hot brines and meteoric groundwater (Liu et al., 2004), a mixture of crust-only and crust–mantle sources (He et al., 2004b), organic matter fluxes and hot brines within a sedimentary basin (Li et al., 2004; He et al., 2009), basinal formation water (Xu et al., 2005), and hot brines within thrust–nappe structures (He et al., 2005).

Here, we present new research into the formation of mineralization within the eastern ore zone of the Baiyangping ore district. This research uses new and previously published fluid inclusions, REE, and S–C–O isotopic data to compare the origins of ore-forming fluids from the eastern and western ore zones of the Baiyangping ore district.

2. Regional and ore district geology

2.1. Location and geological history

The Lanping–Simao Basin is located in the central part of the Sanjiang tectonic belt, within the eastern Indo-Asian collision zone (Luo et al., 1994; Tao et al., 2002; Xue et al., 2002a; Liao and Chen, 2005; Hou et al., 2006, 2007). This area was initially part of a landmass that formed at the end Silurian, during the Proterozoic–Early Paleozoic closure of the Paleo-Tethys Ocean. The Lancangjiang and Jinshajiang oceanic plates subducted eastward and westward, respectively, beneath the Changdu–Lanping–Simao microplate, forming volcanic island arcs along both edges of a microplate that eventually became part of Laurasia when the Paleo-Tethys Ocean closed in the late Permian or Early Triassic as a response to collision between the Yangtze Plate to the east and the Tibet–Yunnan Plate to the west (Luo et al., 1994; Jin et al., 2003; Fig. 1a).

The growth, history and evolution of the Lanping–Simao Basin is long and complex (Luo, 1990; Cong et al., 1993), and the area preserves evidence of three main phases of development from the initial oceanic basin to an intra-continental basin and subsequently to a basin–mountain system (Tao et al., 2002).

2.2. Stratigraphy

The Lanping–Simao Basin (Fig. 1) is essentially an intracontinental terrestrial basin. There are several sedimentary gaps in the stratigraphic sequence within the basin (Qin and Zhu, 1991; Xue et al., 2002b), which consists of, in ascending order, the Upper Triassic Waigucun (T_3w), Sanhedong (T_3s) and Maichuqing (T_3m) formations, followed by a sedimentary hiatus before the Middle Jurassic Huakaizuo (J_2h) and Upper Jurassic Bazhulu (J_3b) formations, the Lower Cretaceous Jingxing (K_1j), Nanxing (K_1n), and Hutousi (K_1h) formations, an Upper Cretaceous hiatus, the Eocene Yunlong (E_1y), Guolang (E_2g), and Baoxiangsi (E_2b) formations, and a non-subdivided Upper Eocene sedimentary sequence (E_3).

2.3. Structures

The thrust–nappe system in the basin is characteristic of the Lanping Fold Belt, which is thought to have formed during Indo–Asian collision and subsequent Paleocene to Eocene oblique convergence (He et al., 2009). Two approximately E–W-striking geological cross-sections across the northern Lanping Basin indicate that the main thrust faults dip to the west and to the east in the western and eastern segments of the basin, respectively. The Lanping–Simao Basin also contains three major, regional-scale faults that strike NNW–SSE: the Jinshajiang–Ailaoshan and Lancangjiang faults along the eastern and western margins of the basin, respectively, and the Lanping–Simao Fault within the center of the basin (Fig. 1a). All of these faults are thought to penetrate deeply into the lower crust and/or upper mantle (Yin et al., 1990; Xue et al., 2002b; Jin et al., 2003), and the basin also contains some blind E–W-trending structures. The tectonic evolution of the Lanping–Simao Basin was controlled by all of these structures (Xue et al., 2002b, 2003).

2.4. Magmatic activity

Paleogene–Neogene alkaline Himalayan intrusions are exposed along the margin of the Lanping–Simao Basin, and Cenozoic igneous rocks are also present within the basin (Xue et al., 2002a,b, 2003, 2006; Fig. 1). These intrusions are thought to be mantle-derived or to have mixed mantle–crust sources. Both the deep crustal-penetrating faulting and the magmatism within the basin are thought to have been controlled by collision between the Indian and Eurasian plates (Yin et al., 1990; Xue et al., 2002b; Jin et al., 2003).

Paleogene ultramafic, mafic, intermediate, and felsic rocks in the basin were intruded or emplaced at about 46.5 Ma, 36.7 Ma, 38.8 Ma (Zhang et al., 2000), and 43 Ma (Zhao, 2006). The felsic rocks are mainly porphyritic granitoids with minor alkaline and nepheline syenite intrusions, whereas volcanic sequences are dominated by olivine basalts, with alkaline basalts, and trachytes (Teng et al., 2001).

3. Geology of the eastern ore zone within the Baiyangping ore district

The Baiyangping Cu–Ag polymetallic ore district is located in the northern part of the Lanping–Simao foreland fold belt, which lies between the Jinshajiang–Ailaoshan and Lancangjiang faults. The location of the eastern and western ore zones is controlled by deep faults, and fold belts in the study area are associated with frequent tectonic activity, complex and diverse geological processes, and repeated magmatism (Fig. 1). The district also records evidence of multiple stages of mineralization involving a wide variety of metals and associated with significantly different petrological characteristics (Yin et al., 1990; Tian, 1997, 1998; Li et al., 1999; Chen et al., 2000; Yang et al., 2003; Xue et al., 2007; He et al., 2009).

The eastern ore zone consists of the Hexi, Xiaquwu, Dongzhiyan, Yanzidong, Huishan, Heishan, and Huachangshan ore blocks, the majority of which are located along the Huachangshan thrust fault (Fig. 2). The dip of E-dipping thrust faults decreases from ~60–70° to 30–40° in the northern segment of the basin with increasing distance westwards from the Huachangshan Fault. Calcite within clastic rocks associated with these faults has twinning, lattice deformation, and anomalous extinction, suggesting transpressional deformation (He et al., 2004a), whereas a C–T diagram of calcite from the Huachangshan Fault indicates that $\sigma 1$ and $\sigma 3$ have average NW–SE and NE–SW orientations, respectively, implying thrusting from the SE to the NW (He et al., 2004a,b, 2009).

The Huachangshan and Shuimofang faults form a nappe front pop-up structure that was not only the main conduit for hydrothermal fluids in this area but also forms the main ore-hosting structure in the mining area. The belt dips generally to the east

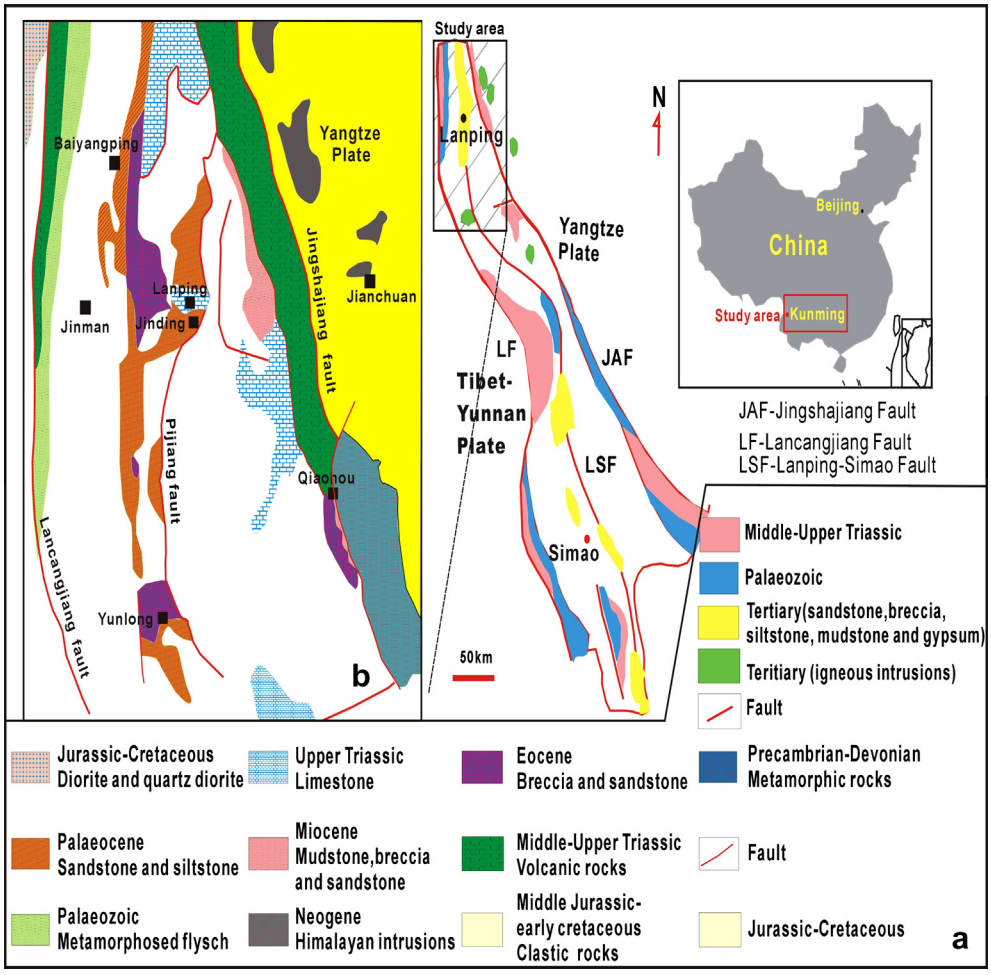

Fig. 1. Location and geology of the Lanping–Simao Fold Belt in the area around Lanping, southern China (after Xue et al., 2007): (a) major structural features and a geological map of the Lanping–Simao Belt and (b) location of ore deposits within the Lanping–Simao Basin.

but locally dips to the west within the Dongzhiyan–Xiaquwu block. The fractured zone associated with these faults is 10–20 m wide, and is lithologically zoned from an inner compressional schistose zone to an outer zone of fractured rock. The majority ore blocks are located along the thrust fault and within zones of fractured hangingwall carbonate sediments (T_3s). Orebodies in the study area are usually truncated by E–W-trending strike-slip faults in the eastern thrust system, indicating that these faults post-date mineralization. A cross-section through an orebody within the Dongzhiyan ore block identifies a second-order F1 fault that generally dips at 35–75° to the SE, and a cross-section through an orebody within the eastern thrust-nappe system is shown in Fig. 3.

Proterozoic to Paleozoic units form the basement of the Lanping–Simao Basin, and the eastern ore belt is hosted by carbonates of the Upper Triassic Sanhedong Formation (T_3s) and sandstones of the underlying Paleocene Yunlong (E_1y) and Eocene Baoxiangsi formations (E_2b). Upper Triassic Sanhedong Formation (T_3s) carbonates form a significant ore horizon in the study area and are composed of a lowermost section of thick gray brecciated limestone, dolomitic limestone, and dolomite, and an uppermost section of gray brecciated siliceous and muddy limestones. Orebodies within the Huishan, Heishan and Huachangshan blocks are hosted by the upper carbonate sequence, whereas the lower carbonate sequence hosts orebodies in the other ore blocks.

The main deposit in the study area consists of at least 20 orebodies that have lengths of 135–3500 m, thicknesses of 2.3–17 m, and depths of ~20–320 m (Chen et al., 2004). The ~25 km long deposit is compositionally zoned from south to north, with Zn–Pb, Zn–Pb–Ag, Cu–Ag, Ag–Cu, and Sr-dominant ore zones (He et al., 2009). Orebodies within the deposit are generally present as veins, networks, and lenses, and change in grades from south to north, with Ag, As, Cd, Pb, Sb, and Zn grades decreasing and Bi and Cu grades increasing from the Huachangshan to Xiaquwu to Dongzhiyan ore blocks in the eastern ore zone (Feng et al., 2011a,b).

Mineralization in the study area is associated with dolomitization, calcification, and silicification alteration, although wall rock alteration within the ore deposit is generally weak, taking the form of calcite, dolomite, azurite, and barite replacement, all of which are closely associated with polymetallic Cu–Ag polymetallic mineralization. Pre-mineralization alteration is restricted to silicification, although local pyrite and fluorite precipitation is also locally present, although the relationship between these styles of alteration and mineralization is not clear (Third Geology and Mineral Resources Survey, 2003).

Ore minerals include sphalerite, galena, pyrite (marcasite), and a number of differing types of Cu sulfide (tetrahedrite, Ag- and As-tetrahedrite, chalcocite, chalcopyrite, and bornite), with minor tenorite, cerussite, smithsonite, azurite, malachite, and covellite, in a calcite, celestine, siderite, dolomite, barite, fluorite, and minor quartz gangue (Chen et al., 2000; He et al., 2009). The eastern ore zone has lower Ag, As, Cd, Pb, Sb, and Zn enrichments than

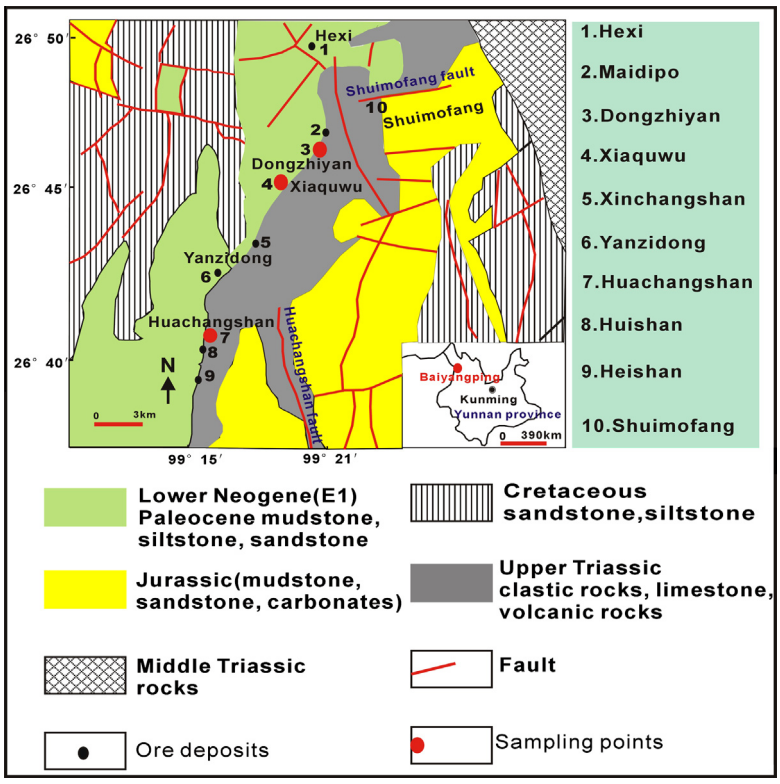

Fig. 2. Simplified geological map of the eastern ore zone of the Baiyangping ore deposits, Yunnan Province, southern China (modified from He et al., 2007).

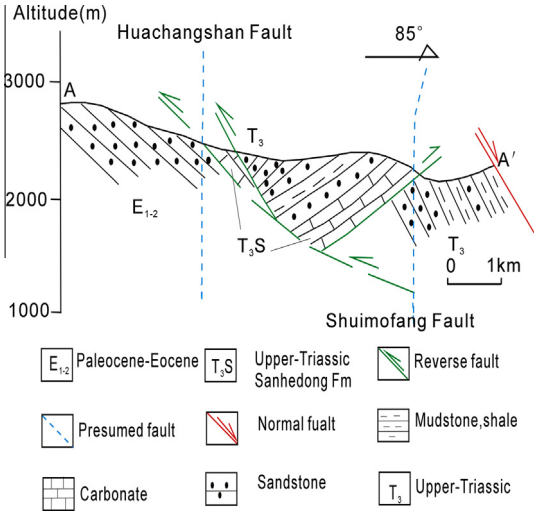

Fig. 3. Geological cross-section through an orebody within the eastern thrust–nappe system (after Third Geology and Mineral Resources Survey, 2003 and He et al., 2009).

elsewhere in the district, and has increasing Bi and Cu enrichments from south to north, with significant Co, Cr, Ni, and V depletions (Feng et al., 2011a,b).

4. Sampling and analytical techniques

4.1. Sampling

Samples were collected from the Sanhedong Formation (T_3s) in the Huachangshan, Xiaquwu, and Dongzhiyan ore blocks within the eastern ore belt of the Baiyangping ore district, Lanping, Yunnan Province, China. Samples were petrographically examined before gangue (calcite and dolomite), ore, and wall rock samples were trimmed to remove altered surfaces, cleaned with deionized water, and crushed and powdered in an agate mill. Doubly-polished calcite and dolomite thin sections were also prepared from the selected samples and examined by standard microscopy before further analysis.

Sulfur isotopic compositions ($\delta^{34}S$) were acquired from fine, granular sphalerite, galena, celestine, tetrahedrite, and pyrite obtained from mineralization stage rocks. Carbon and oxygen isotopic compositions ($\delta^{13}C$ and $\delta^{18}O$) were determined for gangue minerals (calcite and dolomite) in main mineralization stage rocks. Detailed fluid inclusion microthermometric analysis was undertaken on nine coarse-grained calcite and dolomite samples formed during the main stage of mineralization. The sample size was deemed sufficient to characterize the conditions of ore formation as the main stage of mineralization is developed uniformly throughout the eastern ore belt, as deduced from textural and mineral paragenetic relationships between sphalerite, galena, calcite, and dolomite (Fig. 4).

The following textures are present in rocks associated with the main stage of mineralization (Fig. 4): brecciated calcite (a), massive and veinlet calcite and galena (b), massive calcite and sphalerite (c), massive calcite, galena, and sphalerite, veinlet calcite, and massive textured calcite + galena + sphalerite (d, g, h) within the Huachangshan ore block, and veinlet textured dolomite in the Dongzhiyan (i) and Xiaquwu (j), ore blocks, respectively.

4.2. Analytical techniques

4.2.1. Microthermometry

Microthermometric studies were conducted at the State Key Laboratory of Ore Deposit Geochemistry, Institute of Geochemistry, Chinese Academy of Science, Guiyang, China, following procedures

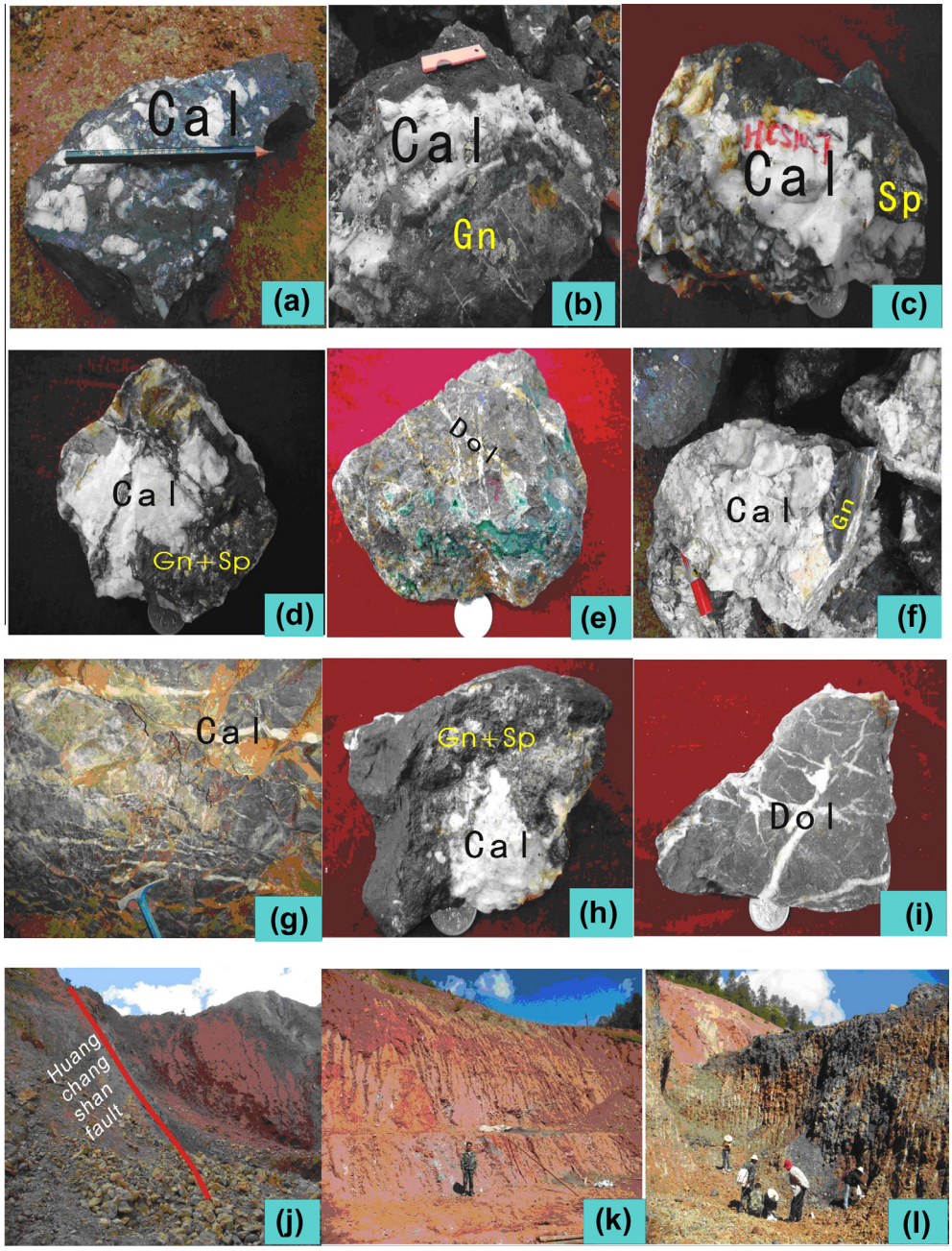

Fig. 4. Mineral textures and sampling sites within the eastern ore zone of the Baiyangping ore district: (a) brecciated texture within Cal. (Huachangshan ore block); (b) massive + veinlet Cal. + Gn. texture (Huachangshan ore block); (c) massive Cal. + Sp. (Huachangshan ore block); (d) massive Cal. + Sp. + Gn. (Huachangshan ore block); (e) veinlet Dol. (Dongzhiyan ore block); (f) massive Cal. + Gn.; (g) veinlet Cal. (Huachangshan ore block); (h) massive Cal. + Gn. + Sp. (Huachangshan ore block); (i) veinlet Dol. (Xiaquwu ore block); (j) Photograph showing the Huachangshan Fault; (k) evaporite sulfate bed and (l) relationship between evaporate sulfate bed and #1 orebody within the Xiaquwu ore block. Cal. = calcite, Gn. = galena, Sp. = sphalerite, Dol. = dolomite.

outlined by Roedder (1984) and Shepherd et al. (1985), and using a Linkam THMGS600 heating–freezing stage. The stage was calibrated against pure H_2O synthetic (0 °C and + 374.1 °C) and pure CO_2-bearing natural inclusions (−56.6 °C). Temperature measurements below 0 °C are accurate to ±0.1 °C, whereas heating runs have temperatures that are accurate to ±1 °C. Salinity data (expressed as wt.% equivalent NaCl) were calculated using the method of Chi and Ni (2007), and this study used the equations of state of Zhang and Frantz (1987) for the H_2O–NaCl ± KCl. A total of 60 freezing and 50 homogenization temperatures are presented during this study, including both new data and data obtained during other recent research (Third Geological Team, 1994; Wei, 2001; He et al., 2004a,b; Zhao, 2006). Fluid inclusion temperatures and salinities are given in Table 1.

4.2.2. Rare earth element geochemistry

Rare earth element (REE) concentrations were determined using a Perkin–Elmer Sciex ELAN 6000 ICP–MS at the State Key Laboratory of Ore Deposit Geochemistry, Institute of Geochemistry, Chinese Academy of Science, Guiyang, China. Powdered samples (50 mg) were dissolved in high-pressure Teflon bombs using an HF + HNO_3 mixture heated for 48 h at ~190 °C (Qi et al., 2000). Rh was used as internal standard to monitor signal drift during counting, and a GBPG-1 international standard was used to

Table 1
Homogenization temperatures and salinities of fluid inclusions from the eastern ore zone of the Baiyangping ore district, Yunnan Province, China; T_i = freezing temperature; T_h = homogenization temperature; Slt = salinity.

Sample no.	Ore block	Host mineral	T_{ht} (°C)	T_i (°C)	Slt (wt.% NaCl eq.)	Sample no.	Ore block	Host mineral	T_i (°C)	T_{ht} (°C)	Slt (wt.% NaCl eq.)
HCS10-1	Huachangshan	Calcite	179	−2.6	4.34	XQW10-21	Xiaquwu	Dolomitized	143	−12.3	16.24
			182	−3.9	6.3			Calcite	131	−13.5	17.34
			130			XQW10-21-1	Xiaquwu		135	−11.9	15.86
			185	−3.6	5.86				168	−12.6	16.53
			172	−4.9	7.73				175	−10.3	14.25
HCS10-1-1	Huachangshan	Calcite	156	−2.6	4.34	XQW10-21-2	Xiaquwu		162		
			155	−3.9	6.3				198		
			149						176		
			148	−3.6	5.86	XQW10-23	Xiaquwu	Dolomitized	166	−10.2	14.15
HCS10-1-2	Huachangshan	Calcite	196	−2.5	4.18			Calcite	166	−12.2	16.15
			199	−3.6	5.86				167		
			101	−4.9	7.73				153	−11.3	15.27
			189	−2.6	4.34				169		
HCS10-28	Huachangshan	Calcite	142	−3.9	6.3	XQW10-33	Dongzhiyan	Dolomite	169	−12.2	16.15
HCS10-6		Calcite	120	−4.2	6.74				152		
			195	−2.3	3.87				189	−10.9	14.87
			123	−4.6	7.31				186		
HCS10-6-1	Huachangshan	Calcite	119	−6.1	9.34				188	−13.6	17.43
			118	−5.5	8.55	HCS10-10	Huachangshan	Calcite	180	−6.1	9.34
			142	−6.4	9.73				162	−2.5	4.18
			175						168	−3.5	5.71
HCS10-6-2	Huachangshan	Calcite	186	−3.6	5.86				160	−3.6	5.86
			125	−2.5	4.18				128	−2.6	4.34
			136	−3.6	5.86	HCS10-10-1	Huachangshan	Calcite	198		
HCS10-15	Huachangshan	Calcite	155	−4.9	7.73				165	−4.9	7.73
			165	−2.6	4.34				186	−2.6	4.34
			138	−3.9	6.3				196	−3.9	6.3
HCS10-15-1	Huachangshan	Calcite	126			HCS10-4	Huachangshan	Calcite	186	−5.6	8.68
			135	−2.6	4.34				169	−6.2	9.47
			133	−3.6	5.86				165	−3.6	5.86
			136	−4.2	6.74				198	−2.6	4.34
HCS10-15-2	Huachangshan	Calcite	128	−3.5	5.71						
			133	−5.3	8.28	After Xu and Li (2003)	Sanshan	Calcite	152–229		3.0–6.4
			162	−6.2	9.47		Ore	Quartz	147–205		4.2–5.2
			126	−3.2	5.26		Block				
HCS10-15-3	Huachangshan	Calcite	138			After Chen et al. (2004)		Quartz	151–239		3.4–16.5
			185					Calcite	114–143		5.7–6.5
			165	−5.5	8.55			Celestite	145		7.3
			160	−5.2	8.14			Quartz	135–184		17.0–17.1
HCS10-15-4	Huachangshan	Calcite	153	−6	9.21			Celestite	106–191		6.8–9.1
			156	−4.2	6.74			Celestite	136–185		6.6–9.0
			165	−3.2	5.26			Sphalerite	115–170		10.0–19.9
			151	−5.5	8.55	After He et al. (2004a,b)	Huishan	Calcite	109–295		2.24–11.03
HCS10-15-5	Huachangshan	Calcite	165	−5.5	8.55		Huachangshan	Calcite	141–241		4.46–11.34
			181	−6	9.21						
		Calcite	189	−5.7	8.81		Yanzidong	Calcite	119–276		5.13–11.23
			188	−5.2	8.14		Dongzhiyan	Celestite	112–275		1.65–9.62
			169	−4.3	6.88		Hexi	Calcite	111–248		1.36–11.23

monitor analytical quality control. The analytical precision was generally better than 5% for all elements, and analysis of international OU-6 and GBPG-1 standards was in agreement with recommended values (Table 2).

4.2.3. Sulfur isotopes

Sulfur isotope analyses were conducted at the State Key Laboratory of Environmental Geochemistry, Institute of Geochemistry, Chinese Academy of Science, Guiyang, using sulfide separates prepared by hand-picking and powdering, before this powdered sample material was enclosed in capsules of high-purity tin foil. These sulfides were flash-combusted in a Euro Vector Elemental Analysis 3000 oven, liberating SO_2 during interaction with an O_2-enriched He gas, before being oxidized with WO_3 at 1030 °C. Measurements were then conducted in a continuous-flow isotope ratio mass spectrometer. GBW04415 and GBW04414 international reference standards were repeatedly measured between sample analyses to monitor analytical precision. All S isotope values are expressed in δ notation relative to the Canyon Diablo troilite (CDT) standard, and the precision of $\delta^{34}S$ measurements is better than ±0.2‰.

4.2.4. Carbon and oxygen isotopes

Carbon and oxygen isotope analyses were undertaken at the Laboratory of Stable Isotope Geochemistry, Institute of Mineral Resources, Chinese Academy of Geological Science, Beijing, China. This analysis used powdered samples that were placed into a vacuum system and heated for 1 h at approximately 300 °C, before being reacted with 100% phosphoric acid for approximately 1 h in an 85–90 °C hot water bath, producing CO that was collected in a cold finger within a liquid N_2 cold-trap. This cold finger sample was moved to an approximately −75 °C alcohol–liquid–N_2 cold-trap bath to gather pure CO_2 (McCrea, 1950), which was then analyzed using a Finnegan MAT-251 mass spectrometer. The resulting C and O isotope compositions are reported using standard V-PDB and V-SMOW notations.

Table 2
Rare earth element concentrations (in ppm) of calcite, wall rock, and ore from the eastern ore zone of the Baiyangping ore district, Yunnan Province, China.

After Feng et al. (2011a,b)	HCS10-1-2	HCS10-4	HCS10-5	HCS10-6	HCS10-7	HCS10-10	HCS10-13	HCS10-14	HCS10-15	HCS10-22	HCS10-23	XQW10-7	XQW10-07-1	XQW10-33	DZY10-48
	Calcite	Calcite	Calcite	Calcite	Huachangshan Calcite	Calcite	Calcite	Calcite	Calcite	Calcite	Calcite	Dolomitized calcite	Xiaquwu Dolomitized calcite	Dolomite+ calcite	Dongzhiyan Dolomitized calcite
ΣREE	6.17	9.88	7.61	7.25	13.2	4.53	10.5	6.64	20.8	3.10	5.07	15.3	18.0	38.9	6.93
LREE/HREE	1.00	1.42	1.19	1.13	1.21	1.05	0.61	1.04	1.20	1.06	0.69	2.96	3.84	3.60	5.59
$(La/Yb)_N$	0.83	1.79	1.14	0.90	1.00	1.16	0.49	0.84	0.87	0.87	0.72	2.70	3.86	3.45	10.7
δEu	0.81	0.79	0.68	0.82	0.84	0.90	0.90	0.79	0.82	2.20	0.77	0.65	0.71	0.76	0.86
δCe	0.81	0.82	0.84	0.82	0.78	0.79	0.79	0.85	0.83	0.74	0.75	1.00	0.99	0.74	0.72
New data	HCS10-2 ore	Huachangshan HCS10-10 Ore	HCS10-12 Ore	XQW10-9 Ore	Xiaquwu XQW10-15 Ore	XQW10-19 Ore	HCS10-9 Wall rock	HCS10-11-1 Wall rock	HCS10-21-1 Wall rock	Huachangshan HCS10-29 Wall rock	XQW10-2 Wall rock	Xiaquwu XQW10-5 Wall rock	XQW10-39 Wall rock	Dongzhiyan XQW10-27 Wall rock	XQW10-33 Wall rock
La	0.82	0.46	0.68	2.41	0.63	15.1	2.07	2.04	6.88	40.4	21.2	5.66	4.35	1.68	2.06
Ce	0.89	0.01	0.25	4.13	0.92	24.3	2.75	2.48	5.54	82.3	41.8	11.7	8.46	3.24	2.48
Pr	0.23	0.01	0.08	0.51	0.13	2.42	0.39	0.41	1.40	9.02	4.87	1.41	0.91	0.40	0.48
Nd	0.92	0.06	0.53	1.88	0.50	8.76	1.33	1.57	6.26	34.50	19.20	5.80	3.37	1.71	2.43
Sm	0.32	0.12	0.36	0.58	0.23	1.50	0.37	0.38	1.52	6.75	3.79	1.34	0.78	0.75	0.74
Eu	0.10	0.02	0.11	0.01	0.01	0.01	0.10	0.08	0.38	1.37	0.70	0.28	0.16	0.20	0.20
Gd	0.39	0.15	0.73	1.13	0.28	3.72	0.48	0.51	2.03	6.42	3.55	1.38	0.85	1.44	1.04
Tb	0.07	0.02	0.14	0.13	0.04	0.21	0.07	0.07	0.30	0.93	0.51	0.20	0.12	0.27	0.17
Dy	0.38	0.15	0.87	0.87	0.29	1.51	0.41	0.48	1.87	5.50	3.07	1.31	0.78	1.84	1.09
Ho	0.07	0.03	0.17	0.17	0.06	0.33	0.09	0.11	0.37	1.10	0.60	0.26	0.16	0.35	0.22
Er	0.17	0.08	0.46	0.49	0.17	1.21	0.32	0.35	1.13	3.42	1.91	0.81	0.55	0.96	0.68
Tm	0.03	0.01	0.06	0.06	0.03	0.17	0.04	0.05	0.14	0.47	0.25	0.11	0.08	0.13	0.08
Yb	0.13	0.07	0.34	0.36	0.14	1.23	0.25	0.32	0.93	3.04	1.62	0.72	0.52	0.70	0.51
Lu	0.02	0.01	0.04	0.05	0.03	0.18	0.04	0.04	0.14	0.47	0.25	0.10	0.08	0.10	0.08
ΣREE	4.54	1.21	4.82	12.8	3.46	60.6	8.71	8.89	28.9	196	103	31.1	21.2	13.8	12.3
LREE/HREE	2.62	1.28	0.71	2.92	2.32	6.09	4.13	3.62	3.18	8.16	7.79	5.36	5.74	1.38	2.17
$(La/Yb)_N$	4.27	4.33	1.35	4.53	3.05	8.32	5.61	4.32	5.01	9.00	8.86	5.33	5.67	1.63	2.74
δEu	0.95	0.59	0.69	0.04	0.13	0.01	0.79	0.61	0.71	0.68	0.62	0.67	0.63	0.61	0.75
δCe	0.49	0.05	0.25	0.89	0.77	0.96	0.73	0.65	0.43	1.03	0.98	0.99	1.01	0.94	0.59

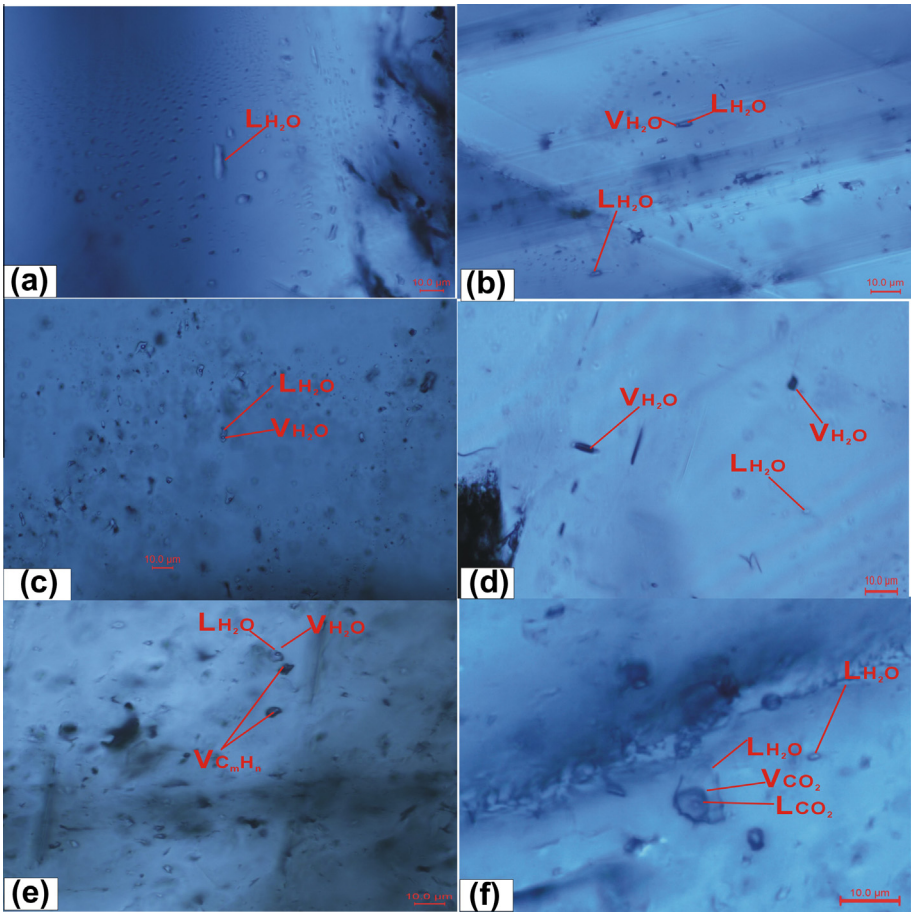

Fig. 5. Photomicrographs of fluid inclusions within representative calcite and dolomite samples collected from the eastern ore belt of the Baiyangping ore district: (a) Type I fluid inclusion (and pseudosecondary fluid inclusions); (b) Type I and II fluid inclusions; (c) Type II fluid inclusions with differing *L*/*V* ratios; (d) coexisting Type III and I fluid inclusions; (e) coexisting Type IV and II fluid inclusions and (f) coexisting Type and I fluid inclusions. Scale bar in each photo represents 10 μm.

5. Results

5.1. Fluid inclusions

5.1.1. Inclusion types

Five inclusion types were identified on the basis of the number of phases observed at room temperature, the degree of filling, and phase variations observed during heating–freezing experiments (Fig. 5). Type I fluid inclusions contain H_2O liquid only, and are the main type of inclusion present in the samples analyzed during this study. These inclusions are generally irregular, range in size from ~5 to 25 μm, and are generally isolated (primary) although less commonly occur as pseudo-secondary trails. Type II inclusions containing H_2O liquid and vapor are also common, and have irregular, rounded, or negative crystal shapes. They are randomly distributed, clustered in the centers of grains, or are present as pseudo-secondary trails, and are similar sizes as the Type I inclusions. Type II inclusions contain vapor phases with volumetric proportions that range between 30% and 70%. Type III fluid inclusions contain only H_2O vapor at room temperature and are minor compared to Type I and II inclusions; they range in diameter from 5 to 15 μm and vary in shape from irregular to ellipsoidal. Type IV fluid inclusions contain pure C_mH_n vapor, are relatively rare, range in diameter from 12 to 20 μm, and vary in shape from irregular to ellipsoidal. Type V fluid inclusions contain aqueous solutions and liquid- or vapor-phase CO_2: H_2O (l) + CO_2 (v) + CO_2 (l). These inclusions are relatively rare, range in diameter from 4 to 30 μm, and vary in shape from irregular to ellipsoidal.

Previous research has also documented fluid inclusions containing CO_2 (l) and aqueous solutions (Xue et al., 2002b), or pure CO_2 (v) (Yang et al., 2003). The fluid inclusion assemblages identified during this study include Type I, II, and III inclusions that are commonly within the same cluster or trail, and Type II inclusions with variable proportions of H_2O liquid and vapor. Daughter minerals were not observed in any of the fluid inclusions. All fluid inclusions are hosted by calcite, whereas dolomite hosts all other types of inclusion.

5.1.2. Homogenization temperatures and salinities

Homogenization temperatures and salinity data for fluid inclusions hosted by calcite, dolomite, dolomitized calcite, quartz, celestine, and sphalerite were compiled from the results of previous studies (Xu and Li, 2003; Chen et al., 2004; He et al., 2004b) and were compared to the analyses undertaken during this study. Fluid inclusion homogenization temperatures range from 101 °C to 295 °C (Table 1), with averages of 158.6 °C for calcite, 176.8 °C for dolomite, 162.2 °C for dolomitized limestone, 151.9 °C for celestite, 172.3 °C for quartz, and 145.6 °C for sphalerite. A stacked histogram clearly shows a single peak in homogenization temperature (Fig. 6); this 120–200 °C peak is dominated by inclusions within calcite, quartz, sphalerite, calcite, dolomitized limestone, and celestine.

Aqueous fluid inclusions have first melting temperatures from −17 °C to −23 °C, indicative of a NaCl–(KCl)–H_2O system. These inclusions have salinities of 1.4–19.9 wt.% NaCl equivalent (Table 1), with modes at approximately 5–10 and 16–21 wt.% NaCl

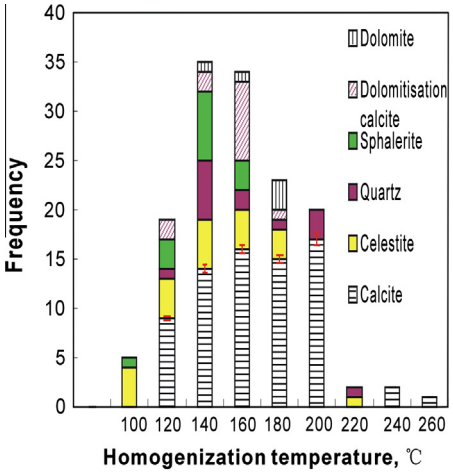

Fig. 6. Homogenization temperatures of fluid inclusions analyzed during this study from the eastern ore zone within the Baiyangping ore district, Yunnan Province, China.

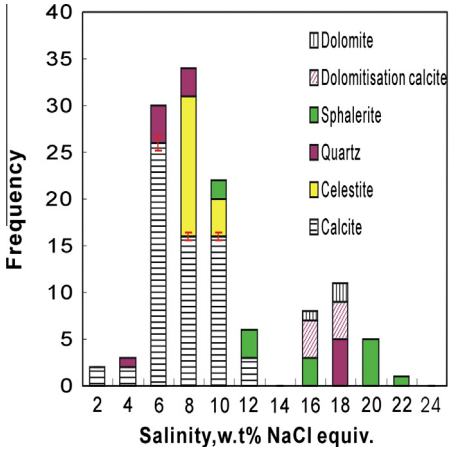

Fig. 7. Fluid inclusion salinities within various minerals from the eastern ore zone of the Baiyangping ore district.

equivalent (Fig. 7), and with average salinities (wt.% NaCl equivalent) of 16.2 for dolomite, 15.7 for dolomitized limestone, 14.3 for sphalerite, 9.9 for quartz, 7.6 for celestite, and 6.5 for calcite; these salinity differences are shown in Fig. 7.

5.2. Rare earth elements (REE)

REE concentrations and chondrite-normalized REE patterns for 45 samples of calcite, dolomite, dolomitized limestone, altered and fresh wall rocks, and ore were compiled from previous studies (Feng et al., 2011a,b) as well as the analyses undertaken during this study. The results are given in Table 2 and Figs 8 and 9.

Calcite, dolomitized calcite, and dolomite samples contain total REE concentrations of 3.10–38.9 ppm, and dolomitized limestones and dolomites have similar left-sloping chondrite-normalized REE distribution patterns that are relatively uncommon for calcite. These samples have $(La/Yb)_N$ values of 2.70–10.7 (dolomitized limestone) and 0.72–2.14 (calcite), and the majority of samples have negative Eu and Ce anomalies, with δEu and δCe values of 0.65–0.90 and 0.74–0.99, respectively (Table 2; Figs 8a and 9a).

Wall rock and ore samples analyzed during this study have total REE concentrations of 1.21–196 ppm (Table 2), and have

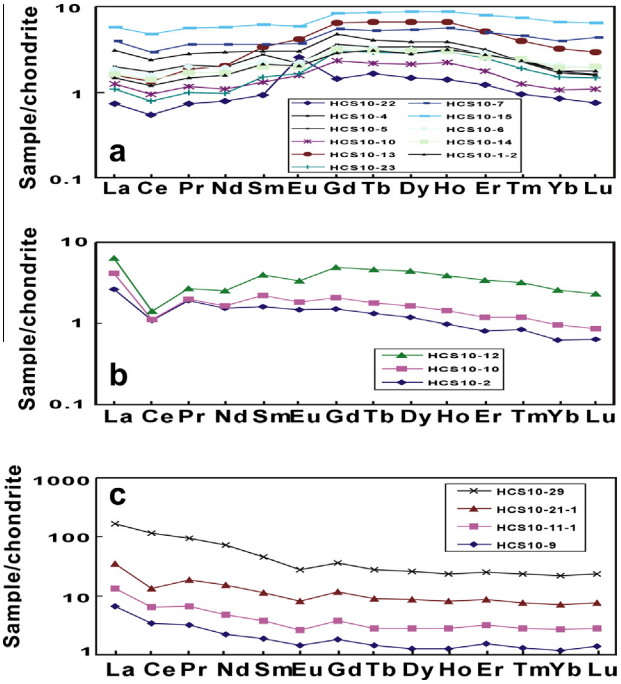

Fig. 8. REE patterns for (a) calcite, (b) ore, and (c) wall rock samples from the Huachangshan ore block within the eastern ore zone of the Baiyangping ore district.

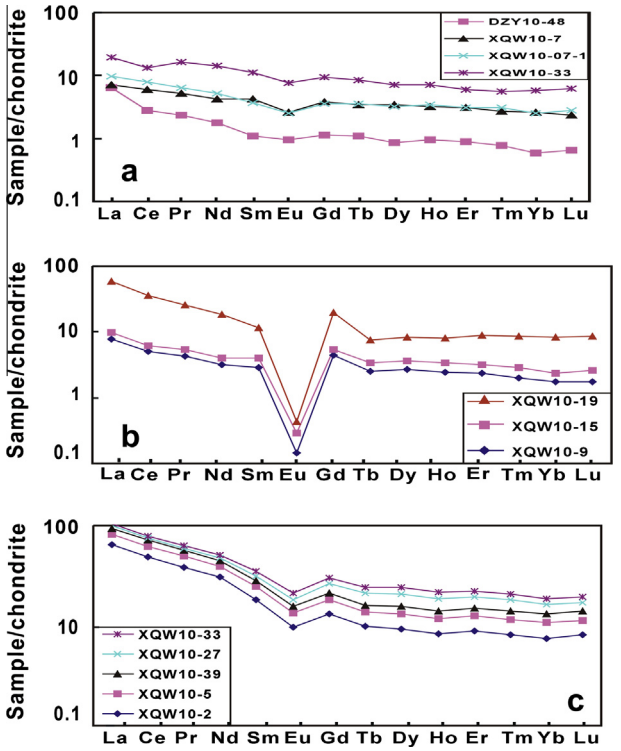

Fig. 9. REE patterns for (a) dolomitized calcite, dolomite (b) ore, and (c) wall rock within the Xiaquwu and Dongzhiyan ore blocks from the eastern ore zone of the Baiyangping ore district.

chondrite-normalized REE distribution patterns that all slope to the right and are enriched in the light rare earth elements (LREEs; Figs 8b and c and 9b and c). These samples have $(La/Yb)_N$ values of 1.35–9.00, and the majority have negative Eu anomalies, with δEu values of 0.01 to 0.95, but with variable negative Ce anomalies and

δCe values of 0.05–0.98, barring for two samples (HCS10–29 and XQW10–39) that have weak positive Ce anomalies (1.03 and 1.01, respectively; Figs 8b and c and 9b and c).

5.3. Isotope data

5.3.1. Sulfur isotopes

The sulfur isotopic compositions of 38 sulfide and sulfate samples (sphalerite, tetrahedrite, galena, pyrite, and celestine) from the eastern ore zone were compiled from both the new data obtained during this study and data from previous studies (Third Geological Team, 1994; Wei, 2001; He et al., 2004b; Zhao, 2006). The results are shown in Table 3 and Fig. 10. Sulfide samples have $\delta^{34}S$ (CDT) of −7.3‰ to 10‰, with a mean of −1.3‰. Sphalerite, pyrite, tetrahedrite, and galena have $\delta^{34}S$ values of −6.3‰ to 2.0‰ (average of 1.43‰), −0.1‰ (single value), −3.2‰ to 1.8‰ (average of −1.4‰), and −7.3‰ to −3.5‰ (average of −4.7‰), respectively. These data show a trend of decreasing $\delta^{34}S$ values from sphalerite > pyrite > tetrahedrite > galena (Fig. 10), indicating that S isotopes were not in overall equilibrium during the formation of the eastern ore zone deposits.

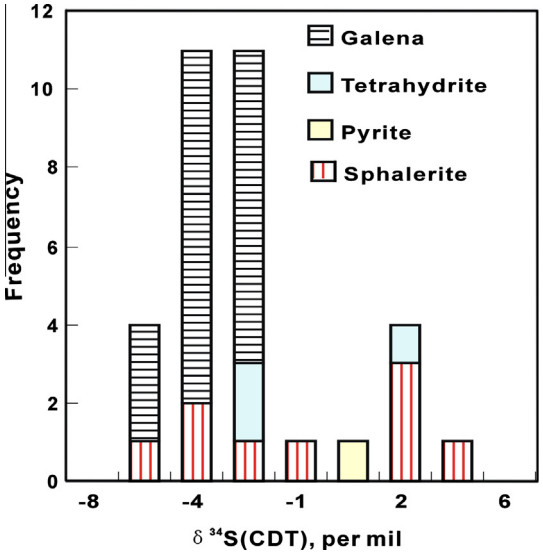

Fig. 10. Frequency distribution plot for sulfur isotopic compositions of samples from the eastern ore zone of the Baiyangping ore district.

5.3.2. Carbon and oxygen isotopes

The carbon and oxygen isotopic compositions of 24 samples (calcite, strontianite, siderite + calcite, mineralized limestone, and limestone) from the eastern ore zone were compiled from previous studies (Chen et al., 2000; Xue et al., 2002b; Xu and Li, 2003; Liu et al., 2004; Zhao, 2006) together with the new data obtained during this study our new data; the results are given in Table 4 and Fig. 11.

The $\delta^{13}C$ (V-PDB) values of the sample range from −8.3‰ to 3.2‰, with a mean of −1.2‰. Calcite, strontianite, siderite + calcite, mineralized limestone, limestone, and dolomite + calcite have $\delta^{13}C$ values of −8.3‰ to 2.7‰ (average of −2.2‰), −5.5‰ (single value), −4.1‰ to 0.7‰ (average of −1.72‰), 1.3–2.1‰ (average of 1.7‰), 2.7–3.2‰ (average of 2.9‰), and 0.9–3‰ (average of 2.1‰), respectively. These samples have $\delta^{18}O$ (V-SMOW) values from 6.46‰ to 24.5‰, with a mean of 15.8‰. Calcite, strontianite, siderite + calcite, mineralized limestone, limestone, and limestone + calcite samples have $\delta^{18}O$ values of 6.5–24.3‰ (average of 16.4‰), 14.1‰ (single value), 8.5–16.4‰ (average of 12.5‰), 9.3–15‰ (average of 11.4‰), 22.7–24.3‰ (average of 23.5‰), and 8.1–24.5‰ (average of 13.5‰), respectively.

These samples have a relatively narrow range of $\delta^{13}C$ values but a much wider range of $\delta^{18}O$ values in a $\delta^{13}C$–$\delta^{18}O$ diagram (Fig. 11); consistent with derivation from marine carbonates.

6. Discussion and conclusions

6.1. Evolution of ore-forming fluids

The evolution of ore-forming fluids is one of the most important subjects in research into carbonate-hosted ore deposit systems. Three phases of mineralization have been identified in the study area: diagenetic, hydrothermal, and supergene. The hydrothermal stage of mineralization is further divided into two stages using primary mineral paragenetic and intergrowth relationships (Fig. 4): an initial sphalerite, dolomitized limestone, and dolomite phase,

Table 3
Sulfur isotopic composition of ore sulfides from the eastern ore zone of the Baiyangping ore district, Yunnan Province, China.

Sample	Mineral	$\delta^{34}S$(CDT)‰	Sample	Mineral	$\delta^{34}S$(CDT)‰
After He et al. (2004a,b)			After	Galena	−3.9
			Wei (2001)	Sphal.	−1.2
HS116	Sphal.	0.1		Sphal.	−4.1
DK-2-1	Pyrite	−0.1		Galena	−3.5
HX-48-1	Sphal.	2.0	After		
HX-48-2	Tetrah.	1.8	Zhao (2006)		
HX-50	Tetrah.	−2.9	DK-2-2	Sphal.	2.1
DK-1	Tetrah.	−3.2	HX-48-1	Sphal.	2
Huishan-1	Galena	−3.7	[a]		
Huishan-1	Galena	−3.9	HCS10-5	Galena	−3.5
Huishan-1	Sphal.	−4.1	HCS10-7-1	Galena	−6.7
After 3rd	Geological		HCS10-7-a	Sphal.	−3.4
Team(1994)			HCS10-8	Galena	−5.5
LD1-2	Galena	−4.0	HCS10-15	Galena	−5.0
LD1-1	Galena	−3.7	HCS10-16	Galena	−4.3
LD1-2-1	Galena	−4.0	HCS10-14-2	Sphal.	−6.3
LD1-1-1	Galena	−7.3	HCS10-22	Galena	−5.0
After	Galena	−4.0	HCS10-25	Galena	−4.8
Wei (2001)	Galena	−7.3	HCS10-26	Galena	−4.8
	Galena	−3.7	HCS10-10	Galena	−4.7

[a] New data obtained during this study.

Table 4
Carbon and oxygen isotopic compositions of hydrothermal carbonates from the eastern ore zone of the Baiyangping ore district, Yunnan Province, China.

Sample	Mineral	$\delta^{13}C$(PDB)‰	$\delta^{18}O$(SMOW)‰	Sample	Mineral	$\delta^{13}C$(PDB)‰	$\delta^{18}O$(SMOW)‰	Sample[a]	Mineral	$\delta^{13}C$(PDB)‰	$\delta^{18}O$(SMOW)‰
After Xue et al. (2002a,b)				After Chen et al. (2000)				HCS10-1-2	Cal.	−2.7	19.3
H-12	Cal.	2.1	20.8	H-53	Sid. + Cal.	−4.1	8.5	HCS10-4	Cal.	−2.7	17.8
H-14	Cal.	2.7	22.6	H-17	Stron.	−5.5	14.1	HCS10-5	Cal.	−3.0	20.1
After Xu and Li (2003)				H-54	Sid. + Cal.	0.7	16.4	HCS10-6	Cal.	−2.7	17.9
S01167	Cal.	−4.6	12.0	H-56	Min. + Lim.	1.3	15	HCS10-7	Cal.	−3.0	17.7
S01172	Cal.	−4.86	9.6	H-60	Min. + Lim.	1.8	10	HCS10-10	Cal.	−2.2	18.6
SS97039	Cal.	2.11	6.5	H-63	Min. + Lim.	2.1	9.3	HCS10-13	Cal.	−1.3	20.7
After Liu et al. (2004)				H-48	Lim.	3.2	24.3	HCS10-14	Cal.	−2.0	19.2
HX-31	Cal.	1.6	9.0	H-66	Lim.	2.7	22.7	HCS10-15	Cal.	−3.3	18.1
HX-32-1	Cal.	−7.6	15.9	H-23	Cal.	0.2	13.1	HCS10-23	Cal.	−2.0	18.5
HX-32-2	Cal.	−7.6	16.0	After Zhao (2006)				XQW10-5	Dol. + Cal.	0.9	8.1
HX-48	Cal.	−3.6	20.3	HCS1-2	Cal.	2.5	10.8	XQW10-7	Dol. + Cal.	2.2	10.6
HX-51	Cal.	−2.4	21.3	After Liu et al. (2004)				XQW10-07-1	Dol. + Cal.	2.3	12.0
HS116	Cal.	0.4	24.3	HXS102	Cal.	−8.3	19.8	XQW10-33	Dol. + Cal.	2.0	12.3
HS101	Cal.	−2.3	16.9	HXS105	Cal.	−3.7	22.7	XQW10-48	Dol. + Cal.	3.0	24.5

[a] Sample = new data obtained during this study; Mineral = host mineral; Cal. = calcite; Stron. = strontianite; Sid = siderite; Min. + Lim. = mineralized limestone; Lim. = limestone; Dol. + Cal. = dolomite + calcite

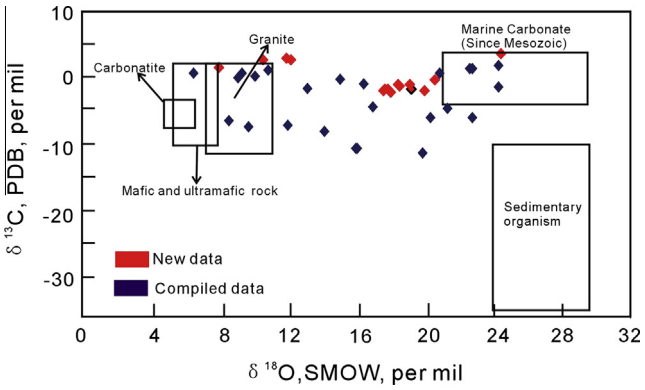

Fig. 11. Diagram showing variations in $\delta^{13}C$ and $\delta^{18}O$ of hydrothermal carbonate minerals from the eastern ore zone of the Baiyangping ore district analyzed during this study; red symbols indicate data generated during this study, blue symbols indicate data from Liu and Liu (1997). (For interpretation of the references to colour in this figure legend, the reader is referred to the web version of this article.)

and a later calcite and celestine phase. The coexistence of different solid/aqueous ratio fluid inclusions in the same cluster indicates inhomogeneity during trapping. No stretching or necking-type fluid inclusions were present in the samples analyzed during this study, and there were no cross-cutting relationships between different fluid inclusion types, suggesting that boiling occurred during mineralization.

6.2. Source(s) of ore-forming fluids and metals

The discussion of the source(s) of ore-forming fluids and metals associated with the formation of the eastern ore zone is based both on previous research (Chen et al., 2000; Yang et al., 2003; He et al., 2004b; Li et al., 2004; Liu et al., 2004; He et al., 2005, 2009) and the new fluid inclusion, REE, and S, C, and O isotope data presented here. The geological and geochemical characteristics of mineral deposits in the study area indicate that two types of fluid were present in the eastern ore zone of the Baiyangping polymetallic ore district during mineralization.

Fluid inclusions are the only direct samples of ore-forming fluids and have been used extensively in research into the origins of mineral deposits (Wilkinson, 2001; Ni et al., 2006; Fan et al., 2006; Chi and Ni, 2007). The presence of saline aqueous fluid inclusions in both ore and gangue minerals with salinities of up to 17.43 wt.% NaCl equivalent (Table 1) is indicative of the involvement of basinal fluids in mineralization. Evaporate sulfates are present throughout Lanping–Simao Basin, suggesting that these basinal brines were derived either from evaporation or from evaporate dissolution (Fig. 4k and l; Xue et al., 2007; He et al., 2009). This previous research, combined with the new data presented here, indicate the presence of at least five types of fluid inclusion within gangue minerals (Gong et al., 2000; Xue et al., 2002b; Yang et al., 2003; Chen et al., 2004; He et al., 2004b). The presence of CO_2-rich inclusions (Fig. 5f; Xue et al., 2002b; Yang et al., 2003; He et al., 2004b) is indicative of a deep (mantle) source for the fluids and metals that were involved in ore formation (Xue et al., 2007; Chi and Xue, 2011). One possible interpretation is that this source may be connected with the eastern thrust–nappe system associated with the Sanshan ore deposits. The front zone within a thrust–nappe system usually generates numerous second-order faults and structural fractures, consequently providing open spaces that allow fluid conduits to converge (He et al., 2009), consistent with observations from the Jinding ore deposit within western Yunnan, China (Xue et al., 2007).

The REE are often used to identify the origin of ore-forming fluids and metals, to trace the evolution of hydrothermal systems, to constrain the conditions of wall rock alteration and ore formation, and to evaluate the genesis of ore deposits (Henderson, 1984; Michard and Albare'de, 1986; Klinkhammer et al., 1994). Dolomitized limestone, dolomite, wall rock, and ore samples from the study area have chondrite-normalized REE patterns that are similar in that they are LREE-rich and slope to the right (Table 2; Figs8a–c and 9a–c). However, these samples have different δEu and δCe values, with ores from the Huachangshan, Xiaquwu and Dongzhiyan ore blocks having highly negative δCe and δEu anomalies (Figs. 8b and 9b). These highly negative values have two possible explanations: firstly, the ore-forming fluid itself may have negative Eu and Ce anomalies associated with changes in geochemical conditions during ore genesis (Lottermoser, 1992; Moller and Morteani, 1983; Mills and Elderfield, 1995; Qi et al., 2008); or secondly, the REE may have been affected by temperature, pH, and Eh conditions and water–rock interaction (Eric et al., 1999). Cerium anomalies are a reliable method to identify any change in the oxidation–reduction conditions of a particular system, as trivalent cerium can easily change to tetravalent cerium in oxidizing conditions, which can then be adsorbed by iron and manganese oxide colloids, resulting in the cerium anomaly typically associated with sea water. In contrast, reducing conditions can lead to both the dissolution of iron and manganese oxides and changing of tetravalent cerium to trivalent cerium, which is subsequently

released (Wang et al., 1999). Negative Ce_N anomalies associated with negative Eu_N anomalies may also indicate a change in redox conditions during fluid ascent, migration, and cooling (Elderfield and Sholkovitz, 1987).

Sulfur within ore-forming fluids can originate from three main sources: (1) a mantle or magmatic source ($\delta^{34}S = 0 \pm 3‰$; Chaussidon and Lorand, 1990), (2) a marine/seawater source ($\delta^{34}S = \pm 20‰$), and (3) reduced sulfur within sediments ($\delta^{34}S < 0$; Rollinson, 1993). The $\delta^{34}S$ values of sphalerite, galena, pyrite, and tetrahedrite range from −7.3‰ to 2.1‰, a wide range that indicates multiple sulfur sources (Table 3; Fig. 10). There are many sources of S in the basin, and a mixture of these sources could also yield near-zero values. This value could be achieved either by mixing of sulfur from different sources, or by variations in the geological conditions of seawater sulfate reduction to sulfur. Ohmoto and Goldhaber (1997) suggest that a value of $\delta^{34}S$ close to zero can be reached by a mechanism that allows deposition of sulfide with the same isotopic composition as the precursor sulfate; this mechanism involves complete reduction of seawater sulfate to sulfur without fractionation in a closed system (Osman et al., 2005).

Samples from the eastern ore zone have a relatively narrow range of $\delta^{13}C$ values but a much wider range of $\delta^{18}O$ values (Fig. 11). In general, the $\delta^{13}C$ values of carbonates should be equal to, or higher than, that of the associated reducing ore-forming fluids (Ohmoto, 1972). Table 4 shows that limestones have $\delta^{13}C$ values that are higher than calcite, and low $\delta^{13}C$ values may indicate the involvement of organic carbon. There are three potential sources of C within ore-forming hydrothermal fluids: (1) a mantle or magmatic source ($\delta^{13}C$ from −5‰ to −2‰ and −9‰ to −3‰, respectively; Taylor, 1986); (2) a marine carbonate source ($\delta^{13}C \approx 0‰$; Veizer et al., 1980); and (3) an organic carbon source ($\delta^{13}C$ from −30‰ to −15‰; Ohmoto, 1972; Ohmoto and Rye, 1979). The $\delta^{13}C$ values for gangue minerals obtained during this study range from −8.3‰ to 2.7‰ (average of 2.09‰), somewhere between the values for mantle and marine sources (Table 4; Fig. 11), indicating the involvement of marine carbonates and a mantle/magmatic derived fluid source within the basin as a source of carbon and oxygen. The presence of hydrocarbon inclusions within both gangue minerals and elsewhere in the basin (e.g., the Jinding deposit; Misra, 2000; Chen and Wang, 2004) suggests that an organic carbon source may be likely. In addition, gangue minerals have $^{18}O/^{16}O$ ratios that range from meteoric values to higher than the values for meteoric water (Misra, 2000), essentially consistent with the ratios of in the Lanping Basin, indicative of a basinal brine source. In addition, the possibility that some of the carbon and oxygen is basin-derived is consistent with the C–O isotope compositions of some hydrothermal carbonates within the Lanping Basin, which in turn are similar to those of marine carbonates.

6.3. Comparison of eastern and western ore zones of the Baiyangping polymetallic ore district

He et al. (2009) compared the characteristics of sediment-hosted Zn–Pb–Cu–Ag ore-forming systems, including sandstone-hosted Pb–Zn (SST), sandstone-hosted Cu (SSC), Mississippi Valley-type (MVT), and sedimentary–exhalative Zn–Pb (SEDEX) deposits, and concluded that the eastern ore zone should be classified as a "Lanping-type" deposit. Here, we use the discussion above and the typical characteristics of "Lanping-type" deposits to compare the ore-forming characteristics of the eastern and western ore zones of the Baiyangping polymetallic ore district.

Tectonically, both the eastern and western ore zones are located in a strongly deformed Paleogene–Neogene foreland basin of the eastern Indo-Asian collision zone (Hou et al., 2006, 2007; Xue et al., 2007). The distribution of ore deposits is controlled by Cenozoic thrust systems related to the ongoing Indo-Asian continent–continent collision that initiated in the Paleocene (Xu and Li, 2003; He et al., 2004b; Xu and Zhou, 2004).

The eastern and western ore zones differ in four respects. First, mineralization in the eastern ore zone is generally hosted by carbonates, whereas mineralization in the western ore zone is hosted by siliciclastic rocks. Second, the majority of mineralization in the eastern ore zone is hosted by the Upper Triassic Sanhedong Formation (T_3s), whereas mineralization in the western ore zone is hosted by the Lower Cretaceous Jingxing (K_1j) and the Middle Jurassic Huakaizuo (J_2h) formations (Third Geology and Mineral Resources Survey, 2003). Third, the eastern zone has, from south to north, Pb–Zn–Ag, Cu–Ag, Ag–(Cu), Pb–Zn–Sr, and Sr assemblages (He et al., 2005), whereas the western ore zone has, from south to north, Pb–Ag–(Zn), Cu–Ag–(Pb), and Cu–(Ag) assemblages (Liu et al., 2010). Fourth, mineralization in the eastern ore zone was generated by the mixing of basinal brines and mantle-derived fluids within the Jinding ore deposits (Xue et al., 2007), whereas the western ore zone developed from basinal fluids only (Xue et al., 2010), forming typical MVT-type deposits.

In summary, organisms, basinal brines, and mantle derived magmas were the primary sources of ore-forming fluids in the eastern ore zone. The eastern and western ore zones of the Baiyangping polymetallic ore district share some similarities with MVT and Lanping-type deposits, but they are significantly different from other sediment-hosted base metal deposit types, such as SEDEX, SST, and SSC deposits. Overall, the eastern ore zone of Baiyangping polymetallic ore district should be considered a "Lanping-type" deposit.

Acknowledgement

This work was funded by the Independent Research fund of the State Key Laboratory of Continental Dynamics (BJ08133-6).

References

Chaussidon, M., Lorand, J.P., 1990. Sulfur isotope composition of orogenic spinel iherzolite massifs from ariege (North-Eastern Pyrencees, France): an ion microprobe study. Geochimica et Cosmochimica Acta 54, 2835–2846.

Chen, K.X., He, L.Q., Yang, Z.Q., Wei, J.Q., Yang, A.P., 2000. Oxygen and carbon isotope geochemistry in Sanshan-Baiyangping copper-silver polymetallogenic enrichment district, Lanping, Yunnan. Geology Mineral Resour. South China 4, 1–8 (in Chinese).

Chen, K.X., Yao, S.Z., He, L.Q., Wei, J.Q., Yang, A.P., Huang, H.L., 2004. Ore-forming fluid in Baiyangping silver-polymetallic mineralization concentration field in Lanping, Yunnan Province. Geological Sci. Technol. Inform. 23, 45–50 (in Chinese with English abstract).

Chen, J., Wang, H.N., 2004. Geochemistry. Science Press, Beijing, p. 129, (in Chinese).

Chi, G.X., Ni, P., 2007. Equations for calculation of NaCl/ ($NaCl + CaCl_2$) ratios and salinities from hydrohalite-melting and ice-melting temperatures in the H_2O–NaCl–$CaCl_2$ system. Acta Petrol. Sinica 23, 33–37.

Chi, G.X., Xue, C.J., 2011. Abundance of CO_2-rich fluid inclusions in a sedimentary basin-hosted Cu deposit at Jinman, Yunnan, China: implications for mineralization environment and classification of the deposit. Mineral. Deposita 46, 365–380.

Cong, B.L., Wu, G.Y., Zhang, Q., Zhang, R.Y., Zhai, M.G., Zhao, D.S., Zhang, W.H., 1993. Tectonic evolution of the paleo-Tethys rock tectonic zone in western Yunnan, China. Sci. China (Series B) 23, 1201–1207 (in Chinese).

Elderfield, H., Sholkovitz, E.R., 1987. Rare earth elements in the pore waters of reducing near shore sediments. Earth Planet. Sci. Lett. 82, 280–288.

Eric, D., Philippe, B., Jean, L.C., 1999. Yttrium and rare earth elements in fluids from various deep-sea hydrothermal systems. Geochim. Cosmochim. Acta 63, 627–643.

Fan, H.R., Hu, F.F., Yang, K.F., Wang, K.Y., 2006. Fluid unmixing/immiscibility as an ore-forming process in the giant REE-Nb-Fe deposit, Inner Mongolian, China: Evidence from fluid inclusion. J. Geochem. Explor. 89, 104–107.

Feng, C.X., Bi, X.W., Wu, L.Y., Zou, Z.C., Tang, Y.Y., 2011a. The significance and REE geochemistry of calcite in the eastern ore belt of the Baiyangping poly-metallic metallogenic area, Northwestern Yunnan Province, China. J. Jinlin Univ. (Earth Science Ed.) 41, 1397–1406 (in Chinese).

Feng, C.X., Bi, X.W., Hu, R.Z., Liu, S., Wu, L.Y., Tang, Y.Y., Zou, Z.C., 2011b. The study on paragenesis-separation mechanism and source of ore-forming element in the Baiyangping Cu–Pb–Zn–Ag polylmetallic ore deposit, Lanping basin, southwestern China. Acta Petrol. Sinica 27, 2604–2609 (in Chinese).

Gong, W.J., Tan, K.X., Li, X.M., Gong, G.L., 2000. Geochemical characteristics of fluid and mechanism for ore formation in the Baiyangping copper–silver deposit, Yunnan. Geotectonica Metall. 24, 175–181 (in Chinese with English abstract).
He, L.Q., Chen, K.X., Yu, F.M., Wei, J.Q., Yang, A.P., Li, H., 2004a. Nappe tectonics and their ore-controlling of Lanping basin in Yunnan Province. Geology Prospect. 40, 7–12 (in Chinese with English abstract).
He, L.Q., Chen, K.X., Wei, J.Q., Yu, F.M., 2005. Geological and geochemical characteristics and genesis of ore deposits in eastern ore belt of Baiyangping area, Yunnan Province. Mineral Deposits 24, 61–70 (in Chinese with English abstract).
He, L.Q., Song, Y.C., Chen, K.X., Hou, Z.Q., Yu, F.M., Yang, Z.S., Wei, J.Q., Li, Z., Liu, Y.C., 2009. Thrust-controlled, sediment-hosted, Himalayan Zn–Pb–Cu–Ag deposits in the Lanping foreland fold belt, eastern margin of Tibetan Plateau. Ore Geol. Rev. 36, 106–132.
He, M.Q., Liu, J.J., Li, C.Y., Li, Z.M., Liu, Y.P., 2004b. Mechanism of ore-forming fluids of the Lanping Pb–Zn–Cu polymetallic mineralized concentration area-an example study on the Baiyangping ore district. Geol. Publ. House, Beijing, 1–117 (in Chinese).
Henderson, P., 1984. Rare Earth Element Geochemistry. Elsevier Science Publishers, Amsterdam.
Hou, Z.Q., Khin, Z., Pan, G.T., Mo, X.X., Xu, Q., Hu, Y.Z., Li, X.Z., 2007. Sanjiang Tethyan metallogenesis in S.W. China: tectonic setting, metallogenic epochs and deposit types. Ore Geol. Rev. 31, 48–87.
Hou, Z.Q., Pan, G.T., Wang, A.J., Mo, X.X., Tian, S.H., Sun, X.M., Ding, L., Wang, E.Q., Gao, Y.F., Xie, Y.L., Zeng, P.S., Qin, K.Z., Xu, J.F., Qu, X.M., Yang, Z.M., Yang, Z.S., Fei, H.C., Meng, X.J., Li, Z.Q., 2006. Metallogenesis in Tibetan collisional orogenic belt: II. Mineralization in late-collisional transformation setting. Mineral Deposits 25, 521–543 (in Chinese with English abstract).
Jin, X.C., Wang, Y.Z., Xie, G.L., 2003. Devonian to Triassic successions of the Changning-Menglian belt, Western Yunnan, China. Acta Geologica Sinca 77, 440–456.
Klinkhammer, G.P., Elderfield, H., Edmond, J.M., Mitra, A., 1994. Geochemical implications of rare earth element patterns in hydrothermal fluids from mid-ocean ridges. Geochim. Cosmochim. Acta 585, 105.
Li, X.Z., Liu, W.J., Wang, Y.Z., Zhu, Q.W., 1999. Tectonic evolution of the Tethys and mineralization in the Sanjiang Region, S.W. China. Geol. Publ. House, Beijing 258 (in Chinese with English abstract).
Li, Z.M., Liu, J.J., Qin, J.Z., Liao, Z.T., Zhang, C.J., 2004. C, O and H isotopic compositions of polymetallic deposits in Lanping basin, western Yunnan Province and their geological significance. J. Jilin Univ. (Earth Science Ed.) 34, 360–366 (in Chinese with English abstract).
Liao, Z.T., Chen, Y.K., 2005. Nature and evolution of Lanping-Simao basin prototype. J. Tongji Univ. (Nature Science) 33, 1528–1531 (in Chinese with English abstract).
Liu, J.J., He, M.Q., Li, Z.M., Liu, Y.P., Li, C.Y., Zhang, Q., Yang, W.G., Yang, A.P., 2004. Oxygen and carbon isotopic geochemistry of Baiyangping silver–copper polymetallic ore concentration area in Lanping basin of Yunnan province and its significance. Mineral Deposits 23, 1–10 (in Chinese with English abstract).
Liu, J.J., Zhai, D.G., Li, Z.M., He, M.Q., Liu, Y.P., Li, C.Y., 2010. Occurrence of Ag Co, Bi and Ni elements and its genetic significance in the baiyangping silver–copper polymetallic metallogenic concentration area, Lanping basin, southwestern China. Acta Petrol. Sinica 26, 1646–1660 (in Chinese with English abstract).
Liu, J.M., Liu, J.J., 1997. Basin fluid genetic model of sediment-hosted micro-disseminated gold deposit in the gold-triangle area, between Guizhou, Guangxi and Yunnan. Acta Mineral. Sinica 17, 448–456 (in Chinese with English abstract).
Lottermoser, B.G., 1992. Rare earth elements and hydrothermal ore formation processes. Ore Geol. Rev. 7, 25.
Luo, J.L., 1990. Basic characteristic and evolution of the Tethys in Western Yunnan, China. Yunnan Geol. 9, 247–280 (in Chinese).
Luo, J.L., Yang, Y.H., Zhao, Z., Chen, J.T., Yang, J.Z., 1994. Evolution of the Tethys in Western Yunnan and Mineralization for Main Metal Deposits. Geological Publishing House, Beijing, pp. 1–340 (in Chinese).
McCrea, J.M., 1950. The isotopic chemistry of carbonates and a paleo-temperature scale. J. Chem. Phys. 18, 849–857.
Michard, A., Albare'de, F., 1986. The REE content of some hydrothermal fluids. Chem. Geol. 55, 51.
Mills, R.A., Elderfield, H., 1995. Rare earth element geochemistry of hydrothermal deposits from the active TAG Mound, 26°N Mid-Atlantic Ridge. Geochim. Cosmochim. Acta 59, 3511–3524.
Misra, K.C., 2000. Understanding Mineral Deposits. Kluwer Academic Publishers, London, p. 845.
Moller, P., Morteani, G., 1983. On the geochemical fractionation of rare earth elements during the formation of Ca-minerals and its application to problem of the genesis of ore deposits. In: Augustithis, S.S. (Ed.), The Significance of Trace Elements in Solving Petrogenetic Problem and Controversies. The ophrastus Pub, Tens, p. 747.
Ni, P., Huang, J.B., Jiang, S.Y., 2006. Infrared fluid inclusion microthermometry on coexisting wolframite and quartz from Dajishan tungsten deposit, JiangXi province, China. Geochim. Cosmochim. Acta 70, 444.
Ohmoto, H., 1972. Systematics of sulfur and carbon isotope in hydrothermal ore deposits. Economic Geol. 675, 51–579.
Ohmoto, H., Rye, R.O., 1979. Isotopes of sulfur and carbon. In: Barnes, H.L. (Ed.), Geochemistry of Hydrothermal Ore Deposits. Wiley, New York, pp. 509–567.
Ohmoto, H., Goldhaber, M.B., 1997. Sulfur and carbon isotopes. In: Barnes, H.L. (Ed.), Geochemistry of Hydrothermal Ore Deposits, third ed. Wiley, New York, pp. 517–611.
Osman, K., Ulvi, U., Ahmet, E., 2005. A study of sulfur isotopes in determining the genesis of Goynuk and Celaldagi Desandre Pb–Zn deposits, eastern Yahyali, Kayseri, Central Turkey. J. Asian Earth Sci. 25, 279–289.
Qi, L., Hu, J., Grégoire, D.C., 2000. Determination of trace elements in granites by inductively coupled plasma mass spectrometry. Talanta 51, 507–513.
Roedder, E., 1984. Fluid inclusions. Mineral. Soc. Am. Rev. Mineral. 12, 644.
Qi, X.X., Yu, F.L., Yu, C.L., 2008. Rare earth element and trace element geochemistry of Shalagang Antimony Deposit in the Southern Tibet and its tracing significance for the origin of metallogenic elements. Geoscience 22, 162–172 (in Chinese with English abstract).
Qin, G.J., Zhu, S.Q., 1991. The ore-forming model of the Jinding lead–zinc deposit and prediction. J. Yunnan Geol. 10, 145–190.
Rollinson, H.R., 1993. Using Geochemical Data: Evalution, Presentation, Interpretation. Longman Scientific and Technical Press, pp. 306–308.
Shao, Z.G., Meng, X.G., Feng, X.Y., Zhu, D.G., 2002. Analysis on the ore-forming geodynamics of the Baiyangping ore-concentrated field, Yunnan Province. Acta Geosci. Sinica 23, 201–206 (in Chinese with English abstract).
Shepherd, T.J., Ranking, A.H., Alderthon, D.H.M., 1985. A Practical Guide to Fluid Inclusion Studies. Blackie and Son, Glasgow and London, p. 239.
Tao, X.F., Zhu, L.D., Liu, D.Z., Wang, G.Z., Li, Y.G., 2002. The formation and evolution of the Lanping basin in western Yunnan. J. Chengdu Univ. Technol. 29, 521–525 (in Chinese with English abstract).
Taylor, B.E., 1986. Magmatic volatiles: isotope variation of C, H and S: stable isotopes in high temperature geological process. Mineral. Soc. Am. Rev. Mineral. 16, 185–226.
Teng, Y.G., Liu, J.D., Zhang, C.J., Ni, S.J., Peng, X.H., 2001. Trace elements characteristic rock series in Lanping basin and its neighbour areas. J. Chengdu Univ. Technol. 28, 40–44 (in Chinese).
Third Geological Team, 1994. The Geological Exploration Report of Lead–zinc Ore Deposit in Lanping Country, Yunnan Province. Unpublished Report, Yunnan Geological and Mineral Resources Bureau, pp. 101–105 (in Chinese).
Third Geology and Mineral Resources Survey, 2003. The Baiyangping Cu–Ag–Pb–Zn–Co mineralized concentration district, Exploration Report, Yunnan Province. Yunnan Geological Survey, pp. 1–266 (in Chinese).
Tian, H.L., 1997. The geological features of Baiyangping Cu–Ag polymetallic deposit, Lanping. J. Yunan Geol. 16, 105–108 (in Chinese).
Tian, H.L., 1998. The geological features of the Sanshan poly-metallic deposit. J. Yunan Geol. 17, 199–206 (in Chinese).
Veizer, J., Holser, W.T., Wilgus, C.K., 1980. Correlation of $^{13}C/^{12}C$ and $^{34}S/^{33}S$ secular variation. Geochim. Cosmochim. Acta 44, 579–588.
Wang, C.S., Hu, X.M., Li, X.H., 1999. Dissolved oxygen in palaeo-ocean: anoxic events and high-oxygen problems. Marine Geol. Quatern. Geol. 19, 39–47.
Wei, J.Q., 2001. S–Pb isotopic geochemistry of copper multi-metal deposits in Hexi, Yunnan province. Geol. Mineral Resour. South China 3, 36–39 (in Chinese with English abstract).
Wilkinson, J.J., 2001. Fluid inclusions in hydrothermal ore deposits. Lithos 55, 229–272.
Xu, Q.D., Li, J.W., 2003. Migration of ore-forming fluids and its relation to zoning of mineralization in northern Lanping Cu-polymetallic area, Yunnan Province: evidence from fluid inclusions and stable isotopes. Mineral Deposits 22, 366–376 (in Chinese with English abstract).
Xu, Q.D., Zhou, L., 2004. Ore-forming fluid migration in relation to mineralization zoning in Cu-polymetallic mineralization district of northern Lanping, Yunnan: evidence from lead isotope and mineral chemistry of ores. Mineral Deposits 23, 452–463 (in Chinese with English abstract).
Xu, S.H., Gu, X.X., Tang, J.X., Chen, J.P., Dong, S.Y., 2005. Stable isotopic geochemistry of three major types of Cu–Ag polymetallic deposits in the Lanping Basin, Yunnan. Bull. Mineral. Petrol. Geochem. 24, 309–316 (in Chinese with English abstract).
Xue, C.J., Chen, Y.C., Yang, J.M., Wang, D.H., 2002a. Analysis of ore-forming background and tectonic system of Lanping basin, Western Yunnan Province. Mineral Deposits 21, 36–44 (in Chinese with English abstract).
Xue, C.J., Chen, Y.C., Yang, J.M., Wang, D.H., 2002b. The CO_2-rich and hydrocarbon-bearing ore-forming fluid and their metallogenic role in the Lanping Pb–Zn–Ag–Cu ore-field, Northwestern Yunnan, China. Acta Geol. Sinica 76, 244–253 (in Chinese with English abstract).
Xue, C.J., Chen, Y.C., Yang, J.M., Wang, D.H., Yang, W.G., Zeng, R., 2003. Geology and isotopic composition of helium, neon, xenon and metallogenic age of the Jinding and Baiyangping ore deposits, northwest Yunnan, China. Sci. China (Series D) 33, 315–322 (in Chinese).
Xue, C.J., Zeng, R., Gao, Y.B., Zhu, H.P., Zhao, S.H., Li, Y.Q., 2006. Fluid process of a heavy metallogenesis at Jinding, Lanping SW-China. Acta Petrol. Sinica 22, 1031–1039.
Xue, C.J., Zeng, R., Liu, S.W., Chi, G.X., Qing, H.R., Chen, Y.C., Yang, J.M., Wang, D.H., 2007. Geologic, fluid inclusion and isotopic characteristics of the Jinding Zn–Pb deposit, western Yunnan, South China: a review. Ore Geol. Rev. 31, 337–359.
Xue, W., Xue, C.J., Chi, G.X., Shi, H.G., Gao, B.Y., Yang, S.F., 2010. Study on the fluid inclusions of Baiyangping poly-metallic deposit in Lanping Basin, northwestern Yunnan, China. Acta Petrol. Sinica 26, 1773–1784.
Yang, W.G., Yu, X.H., Li, W.C., Dong, F.L., Mo, X.X., 2003. The characteristics of metallogenic fluids and metallogenic mechanism in Baiyangping silver and

polymetallic mineralization concentration area in Yunnan Province. Geoscience 17, 27–33 (in Chinese with English abstract).

Yin, H.H., Fan, W.M., Lin, G., 1990. Deep factors on the Lanping-Simao basin evolution and the mantle–crust complex mineralisations. Tectonic Metall. 4, 113–124 (in Chinese with English abstract).

Zhang, Y.G., Frantz, J.D., 1987. Determination of the homogenization temperatures and densities of supercritical fluids in the system NaCl–KCl–$CaCl_2$–H_2O using synthetic fluid inclusions. Chem. Geol. 64, 335–351.

Zhang, C.J., Ni, S.J., Teng, Y.G., Peng, X.H., Liu, J.D., 2000. Relationship between Himalayan tectonic magmatic movement and mineralization in Lanping Basin, Yunnan Province. J. Mineral. Petrol. 20, 35–39 (in Chinese with English abstract).

Zhao, H.B., 2006. Study on the Characteristics and Metallogenic Condition of Copper-Polymetallic Deposits in Middle-northern Lanping Basin, Western Yunnan. Unpublished PhD. Dissertation, China University of Geosciences (in Chinese with English abstract).